



Journal of Cellular Physiology

## Adenovirus-mediated *hPNPase<sup>old-35</sup>* gene transfer as a therapeutic strategy for neuroblastoma

Journal:	<i>Journal of Cellular Physiology</i>
Manuscript ID:	JCP-08-0476.R1
Wiley - Manuscript type:	Original Research Article
Date Submitted by the Author:	24-Dec-2008
Complete List of Authors:	<p>Van Maerken, Tom; Virginia Commonwealth University, Department of Human and Molecular Genetics; Virginia Commonwealth University, Massey Cancer Center; Ghent University Hospital, Center for Medical Genetics; Ghent University Hospital, Department of Clinical Chemistry, Microbiology and Immunology</p> <p>Sarkar, Devanand; Virginia Commonwealth University, Department of Human and Molecular Genetics; Virginia Commonwealth University, Massey Cancer Center; Virginia Commonwealth University, VCU Institute of Molecular Medicine</p> <p>Speleman, Frank; Ghent University Hospital, Center for Medical Genetics</p> <p>Dent, Paul; Virginia Commonwealth University, Massey Cancer Center; Virginia Commonwealth University, VCU Institute of Molecular Medicine; Virginia Commonwealth University, Department of Biochemistry and Molecular Biology</p> <p>Weiss, William; University of California San Francisco, Department of Neurology</p> <p>Fisher, Paul; Virginia Commonwealth University, Department of Human and Molecular Genetics; Virginia Commonwealth University, Massey Cancer Center; Virginia Commonwealth University, VCU Institute of Molecular Medicine</p>
Key Words:	hPNPaseold-35, gene therapy, neuroblastoma, apoptosis, PEG-3 promoter



1  
2  
3 **Adenovirus-mediated *hPNPase*<sup>old-35</sup> gene transfer as a therapeutic strategy for**  
4 **neuroblastoma**  
5  
6  
7  
8  
9

10 Tom Van Maerken,<sup>1,2,3,4</sup> Devanand Sarkar,<sup>1,2,5</sup> Frank Speleman,<sup>3</sup> Paul Dent,<sup>2,5,6</sup> William  
11 A. Weiss,<sup>7</sup> Paul B. Fisher<sup>1,2,5\*</sup>  
12  
13  
14  
15  
16

17 <sup>1</sup>Department of Human and Molecular Genetics, Virginia Commonwealth University,  
18 School of Medicine, Richmond, Virginia  
19

20 <sup>2</sup>Massey Cancer Center, Virginia Commonwealth University, School of Medicine,  
21 Richmond, Virginia  
22  
23  
24  
25  
26

27 <sup>3</sup>Center for Medical Genetics, Ghent University Hospital, Ghent, Belgium  
28

29 <sup>4</sup>Department of Clinical Chemistry, Microbiology and Immunology, Ghent University  
30 Hospital, Ghent, Belgium  
31  
32  
33

34 <sup>5</sup>VCU Institute of Molecular Medicine, Virginia Commonwealth University, School of  
35 Medicine, Richmond, Virginia  
36  
37  
38

39 <sup>6</sup>Department of Biochemistry and Molecular Biology, Virginia Commonwealth  
40 University, School of Medicine, Richmond, Virginia  
41  
42

43 <sup>7</sup>Department of Neurology, University of California San Francisco, San Francisco,  
44 California  
45  
46  
47  
48  
49

50 **\*Correspondence to:** Paul B. Fisher, Department of Human and Molecular Genetics,  
51 Massey Cancer Center, VCU Institute of Molecular Medicine, Virginia Commonwealth  
52 University, School of Medicine, Sanger Hall Building 11-015, 1101 East Marshall Street,  
53  
54  
55  
56  
57  
58  
59  
60

1  
2  
3 Richmond, VA 23298. Phone: 804-828-9632; Fax: 804-827-1124; E-mail:  
4  
5 pbfisher@vcu.edu.  
6  
7  
8  
9

10 **Running title:** *hPNPase*<sup>old-35</sup>-based gene therapy for neuroblastoma  
11  
12  
13

14  
15 **Keywords:** *hPNPase*<sup>old-35</sup>, gene therapy, neuroblastoma, apoptosis, *PEG-3* promoter  
16  
17

18  
19  
20 **Number of figures:** 6  
21  
22

23  
24 **Number of tables:** 1  
25  
26  
27  
28  
29  
30  
31  
32  
33  
34  
35  
36  
37  
38  
39  
40  
41  
42  
43  
44  
45  
46  
47  
48  
49  
50  
51  
52  
53  
54  
55  
56  
57  
58  
59  
60

**Abstract**

Current treatment options for neuroblastoma fail to eradicate the disease in the majority of high-risk patients, clearly mandating development of innovative therapeutic strategies. Gene therapy represents a promising approach for reversing the neoplastic phenotype or driving tumor cells to self-destruction. We presently studied the effects of adenovirus-mediated gene transfer of human polynucleotide phosphorylase (*hPNPase<sup>old-35</sup>*), a 3',5'-exoribonuclease with growth-inhibitory properties, in neuroblastoma cells. Transgene expression was driven by either the cytomegalovirus (CMV) promoter or by a tumor-selective promoter derived from Progression Elevated Gene-3 (*PEG-3*). Our data demonstrate that efficient adenoviral transduction of neuroblastoma cells and robust transgene expression are feasible objectives, that the *PEG-3* promoter is capable of selectively targeting gene expression in the majority of neuroblastoma cells, and that *hPNPase<sup>old-35</sup>* induces profound growth suppression and apoptosis of malignant neuroblastoma cells, while exerting limited effects on normal neural crest-derived melanocytes. These findings support future applications of *hPNPase<sup>old-35</sup>* for targeted gene-based therapy of neuroblastoma and suggest that combination with the *PEG-3* promoter holds promise for creating a potent and selective neuroblastoma therapeutic.

## Introduction

Successful treatment of high-risk neuroblastoma remains a major challenge in pediatric oncology. This neural crest-derived malignancy accounts for approximately 15% of all childhood cancer mortality in the US (Maris et al., 2007). Clinical and biological characteristics, such as age at diagnosis, disease stage, histopathology, tumor cell DNA content (ploidy), and copy number status of the *N-myc* oncogene, allow for stratification of neuroblastoma patients into different risk groups (Brodeur, 2003; Maris et al., 2007). About half of all cases are currently classified as high-risk disease, with a mortality rate exceeding 60%, pointing at a compelling need to develop alternative treatment strategies (Maris et al., 2007).

An intriguing therapeutic opportunity for a number of human diseases may be offered by a group of ribonucleases endowed with cytotoxic, immunosuppressive, antitumor, angiogenic, and aspermatogenic activities. These enzymes are referred to as Ribonucleases with Special Biological Actions or RISBASEs (D'Alessio, 1993), as their functions extend beyond the processing and turnover of cellular RNA and the breakdown of dietary RNA. Such specialized ribonucleases are present from prokaryotes to higher mammals and operate in a variety of biological processes, including interstrain competition in bacteria, prevention of self-pollination in plants, pathogen survival within host tissues, antiparasitic, antifungal and antiviral defense, neovascularization, and antitumor action (D'Alessio, 1993; Youle et al., 1993). Interestingly, two of the best-studied antitumor ribonucleases, onconase and bovine seminal ribonuclease, have shown

1  
2  
3 profound activity against neuroblastoma both *in vitro* and *in vivo*, even in a context of  
4  
5 resistance to conventional chemotherapeutic agents (Cinatl et al., 1999, 2000; Kotchetkov  
6  
7 et al., 2000; Michaelis et al., 2007). The molecular basis underlying the cytotoxicity of  
8  
9 these ribonucleases is not fully understood, but it is accepted that this activity requires  
10  
11 interaction with the cell membrane, internalization by endocytosis, translocation to the  
12  
13 cytosol, resistance to the endogenous ribonuclease inhibitor (RI) in the cytosol as well as  
14  
15 to extracellular and intracellular proteases, and cleavage of cellular RNA (Benito et al.,  
16  
17 2005; Arnold and Ulbrich-Hofmann, 2006). Onconase is the only ribonuclease hitherto  
18  
19 evaluated in clinical trials, with promising results (Beck et al., 2008), although some  
20  
21 caution is warranted in view of a relatively high renal uptake compared to other  
22  
23 ribonucleases (Vasandani et al., 1996) and evidence of acute multifocal proximal renal  
24  
25 tubular necrosis in mice treated with onconase (Vasandani et al., 1999).  
26  
27  
28  
29  
30  
31  
32  
33

34 We previously identified an evolutionary conserved 3',5'-exoribonuclease, human  
35  
36 polynucleotide phosphorylase (*hPNPase<sup>old-35</sup>*), in an overlapping-pathway screen (OPS)  
37  
38 aimed at delineation of genes displaying coordinated changes in expression during  
39  
40 terminal differentiation of human melanoma cells and cellular senescence of progeroid  
41  
42 fibroblasts (Leszczyniecka et al., 2002). Overexpression of *hPNPase<sup>old-35</sup>* in both  
43  
44 processes suggested implication in regulation of cellular growth, and subsequent studies  
45  
46 documented a potent and widely applicable growth-inhibitory activity. *hPNPase<sup>old-35</sup>* is  
47  
48 an early IFN- $\alpha/\beta$  response gene (Leszczyniecka et al., 2002, 2003), and has been shown  
49  
50 to play a pivotal role in IFN- $\beta$ -induced growth inhibition by a remarkable ability to  
51  
52 specifically degrade *c-myc* mRNA (Sarkar et al., 2006). Transduction of normal human  
53  
54  
55  
56  
57  
58  
59  
60

1  
2  
3 melanocytes with an *hPNPase*<sup>old-35</sup>-encoding non-replicating adenovirus induces a  
4  
5 growth arrest with distinctive morphological and biochemical characteristics of  
6  
7 senescence (Sarkar and Fisher, 2006). In melanoma cells, adenoviral overexpression of  
8  
9 *hPNPase*<sup>old-35</sup> not only provokes a G<sub>1</sub> cell cycle arrest and senescence, but also a  
10  
11 pronounced degree of apoptosis (Sarkar et al., 2003). The growth-suppressive effect of  
12  
13 *hPNPase*<sup>old-35</sup> was similarly observed in breast, colon, prostate and pancreatic carcinoma,  
14  
15 glioblastoma multiforme, fibrosarcoma, and osteosarcoma (Sarkar et al., 2003; and data  
16  
17 not shown). Upregulation of *hPNPase*<sup>old-35</sup> might also mediate chronic inflammatory  
18  
19 pathological processes during aging (Sarkar et al., 2004). The RNase PH (RPH) domains  
20  
21 of *hPNPase*<sup>old-35</sup> are critical in mediating its phenotypic effects (Sarkar et al., 2005).  
22  
23 Multiple molecular mechanisms seem to play a role in the growth-inhibitory and  
24  
25 proinflammatory activity, including selective degradation of *c-myc* mRNA (Sarkar et al.,  
26  
27 2003, 2006), activation of double-stranded RNA-dependent protein kinase (PKR) (Sarkar  
28  
29 et al., 2007), and generation of reactive oxygen species with subsequent NF-κB activation  
30  
31 (Sarkar et al., 2004).  
32  
33  
34  
35  
36  
37  
38  
39  
40

41 The present study explores if *hPNPase*<sup>old-35</sup> could be exploited as a selective and  
42  
43 efficacious tool for gene therapy of neuroblastoma. This strategy was pursued using  
44  
45 replication-incompetent adenoviruses in which *hPNPase*<sup>old-35</sup> expression is driven by the  
46  
47 CMV minimal promoter (Ad.CMV-*hPNPase*<sup>old-35</sup>) or by the minimal promoter region of  
48  
49 Progression Elevated Gene-3, *PEG-3* (Ad.PEG-*hPNPase*<sup>old-35</sup>). The *PEG-3* promoter was  
50  
51 found previously to function selectively in diverse cancer cells with limited activity in  
52  
53 normal cells, and hence has the potential of cancer-specific targeting of transgene  
54  
55  
56  
57  
58  
59  
60

1  
2  
3  
4  
5  
6  
7  
8  
9  
10  
11  
12  
13  
14  
15  
16  
17  
18  
19  
20  
21  
22  
23  
24  
25  
26  
27  
28  
29  
30  
31  
32  
33  
34  
35  
36  
37  
38  
39  
40  
41  
42  
43  
44  
45  
46  
47  
48  
49  
50  
51  
52  
53  
54  
55  
56  
57  
58  
59  
60

expression (Su et al., 2005). Our results lend support to the potential use of adenovirus-based *hPNPase<sup>old-35</sup>* delivery in the treatment of neuroblastoma.

For Peer Review



## Materials and Methods

### Cell lines and culture conditions

Human neuroblastoma cell lines IMR-32, NGP, SHEP and SK-N-SH were kindly provided by Dr. R. Versteeg (University of Amsterdam, The Netherlands), and SK-N-BE(2c) human neuroblastoma cells by Dr. J. Lunec (University of Newcastle, UK). Human DU-145 prostate carcinoma cells were purchased from the American Type Culture Collection (Manassas, VA). An SV40 T-antigen immortalized human foreskin melanocyte cell line, FM-516-SV, was initially provided by Dr. L. Diamond (Wistar Institute, PA). The present studies used a subclone of FM-516-SV cells (Sarkar et al., 2006). All cells were cultured as described (Van Maerken et al., 2006).

### Adenoviral vector construction, virus production and infection protocol

The recombinant replication-defective adenoviruses, Ad.CMV-*GFP* (green fluorescence protein [GFP] expression driven by CMV promoter), Ad.CMV-*hPNPase*<sup>old-35</sup> (hemagglutinin [HA]-tagged *hPNPase*<sup>old-35</sup> expression driven by CMV promoter), and Ad.PEG-*hPNPase*<sup>old-35</sup> (HA-tagged *hPNPase*<sup>old-35</sup> expression driven by *PEG-3* promoter), were created by cloning the transgene into a shuttle vector followed by homologous recombination in *E. coli* of the shuttle vector with an adenoviral vector in which the E1 and E3 regions have been deleted, as described previously (Leszczyniecka et al., 2002; Holmes et al., 2003). Production of viral particles in HEK293 cells, virus purification, and titration were performed as described (Holmes et al., 2003). Adenoviral infection of cells, 24 h after plating, was performed at the indicated multiplicity of infection (MOI) in

1  
2  
3 a minimal volume of serum-free RPMI 1640 medium for 3 h at 37 °C, with rocking of  
4  
5 the plates every 15 min, followed by replenishment of complete medium and incubation  
6  
7 at 37 °C for the indicated times. The empty adenoviral vector, *Ad.vec*, was used as a  
8  
9 control.  
10

### 11 12 13 14 15 **Flow cytometric analysis of GFP expression**

16  
17 Cells were seeded in 6-well plates ( $2.5 \times 10^5$  cells per well), incubated for 24 h, and  
18  
19 infected with *Ad.CMV-GFP* at an MOI of 0, 12.5, 25, 50, 100 or 200 plaque-forming  
20  
21 units (pfu) per cell. After 24 h, cells were harvested by trypsinization, washed with  
22  
23 phosphate-buffered saline (PBS), and analyzed for the expression of GFP on a  
24  
25 FACSCalibur flow cytometer (BD Biosciences, San Jose, CA) equipped with CellQuest  
26  
27 Pro acquisition and analysis software version 5.2 (BD Biosciences). The percentage of  
28  
29 GFP-positive cells was quantified using FlowJo version 8.5.3 for Macintosh (Tree Star,  
30  
31 Ashland, OR).  
32  
33  
34  
35  
36  
37  
38

### 39 **Detection of coxsackie-adenovirus receptors (CAR) on the cell surface**

40  
41 Quantification of surface expression of CAR was performed as described previously  
42  
43 (Lebedeva et al., 2002). Briefly, cells were incubated with mouse monoclonal anti-CAR  
44  
45 antibody for 1 h at 37 °C (1:1000 dilution; Millipore, Billerica, MA), washed, exposed to  
46  
47 fluorescein isothiocyanate (FITC)-conjugated anti-mouse immunoglobulins (1:1000  
48  
49 dilution; Sigma, St. Louis, MO) for 1 h at 37 °C in the dark, washed again, and analyzed  
50  
51 on a FACSCalibur using CellQuest Pro version 5.2 (BD Biosciences). Unstained cells,  
52  
53 cells stained with secondary antibody only, and cells incubated with isotype control  
54  
55  
56  
57  
58  
59  
60

1  
2  
3 primary antibody followed by secondary antibody were used as controls. Acquired data  
4  
5 were analyzed in FlowJo version 8.5.3 for Macintosh (Tree Star) using two evaluation  
6  
7 methods. The peak shift was calculated as the difference in peak channels between the  
8  
9 cells stained with anti-CAR antibody and the control cells with the highest FITC signal  
10  
11 intensity, relative to the position of the peak channel of these control cells. The second  
12  
13 method used the Kolmogorov-Smirnov two-sample test for analysis of the flow  
14  
15 cytometric histograms (Young, 1977). This test computes, starting from the histograms,  
16  
17 the cumulative distribution function of fluorescence intensity for each sample and  
18  
19 determines the difference between the cumulative distribution functions, with the *D* value  
20  
21 indicating the greatest difference between the two curves.  
22  
23  
24  
25  
26  
27  
28

### 29 **Analysis of the number of viable cells**

30  
31 Cells were seeded in 96-well tissue culture plates ( $5 \times 10^3$  cells per well), incubated for  
32  
33 24 h, and infected in quadruplicate wells with different adenoviruses at 100 pfu/cell. At 1,  
34  
35 3 and 5 days postinfection, the medium was carefully replaced by fresh medium  
36  
37 containing 0.5 mg/mL MTT (Calbiochem, San Diego, CA), followed by incubation of the  
38  
39 cells at 37 °C for 4 h and then addition of an equal volume of solubilization solution  
40  
41 (0.01 HCl in 10% sodium dodecyl sulfate [SDS]) to each well. The absorbance of the  
42  
43 wells was read at 595 nm with a Bio-Rad Model 550 microplate reader (Bio-Rad,  
44  
45 Hercules, CA). Each condition was tested in three independent experiments.  
46  
47  
48  
49  
50  
51  
52

### 53 **Cell cycle and hypodiploidy analysis**

1  
2  
3 Cells were plated in 10-cm dishes ( $1 \times 10^6$  cells per dish) and infected the next day with  
4 different adenoviruses at 100 pfu/cell. Measurement of cell cycle phase distribution and  
5 hypodiploid DNA content was performed at 2, 3, 4 and 5 days postinfection. Cells were  
6 trypsinized, washed  $2 \times$  with PBS, and fixed in 70% ethanol overnight at  $-20^\circ\text{C}$ . The  
7 cells were subsequently washed  $2 \times$  with PBS, treated with 0.5 mg/mL RNase A at  $37^\circ\text{C}$   
8 for 30 min, and incubated with 0.1 mg/mL propidium iodide at room temperature for 30  
9 min. Cellular DNA content was measured with a FACSCalibur using CellQuest Pro  
10 version 5.2 (BD Biosciences). Cell cycle fractions and the apoptotic  $A_0$  population were  
11 quantified using FlowJo version 8.5.3 for Macintosh (Tree Star).  
12  
13  
14  
15  
16  
17  
18  
19  
20  
21  
22  
23  
24  
25  
26

### 27 **Analysis of caspase-3 and caspase-7 activity**

28  
29 Cells were seeded in 96-well tissue culture plates ( $5 \times 10^3$  cells per well), incubated for  
30 24 h, and infected in triplicate wells with different adenoviruses at 100 pfu/cell. The  
31 combined activity of caspase-3 and caspase-7 was measured at 2 and 3 days postinfection  
32 using the Caspase-Glo 3/7 assay (Promega, Madison, WI) and a Modulus microplate  
33 luminometer (Turner BioSystems, Sunnyvale, CA).  
34  
35  
36  
37  
38  
39  
40  
41  
42  
43

### 44 **Western blot analysis**

45  
46 Protein lysates were prepared on ice in RIPA buffer (Sigma) containing protease and  
47 phosphatase inhibitor cocktails (Roche, Mannheim, Germany), and clarified by  
48 centrifugation at  $16,000 \times g$  for 15 min at  $4^\circ\text{C}$ . Protein concentrations were determined  
49 using the Bradford assay (Bio-Rad). Aliquots containing 25  $\mu\text{g}$  of total protein were  
50 resolved by electrophoresis on 8% SDS-polyacrylamide gels, transferred to 0.2  $\mu\text{m}$   
51  
52  
53  
54  
55  
56  
57  
58  
59  
60

1  
2  
3 nitrocellulose membranes (Pall Corporation, East Hills, NY), and probed with mouse  
4  
5 monoclonal antibodies against HA (1:2000 dilution; Covance, Berkeley, CA) and EF1 $\alpha$   
6  
7 (1:1000 dilution; Millipore). Horseradish peroxidase (HRP)-conjugated goat anti-mouse  
8  
9 immunoglobulins (1:5000 dilution; Sigma) were used as secondary antibodies. Bands  
10  
11 were visualized using ECL Plus detection reagents (Amersham Biosciences, Piscataway,  
12  
13 NJ) according to the manufacturer's instructions.  
14  
15  
16

### 17 18 19 **Real-time quantitative reverse transcription-polymerase chain reaction (RT-PCR)**

20  
21 Total RNA was extracted from cells using the RNeasy Mini Kit (Qiagen, Valencia, CA),  
22  
23 with RNase-free DNase I treatment on column. After an additional RQ1 DNase treatment  
24  
25 in solution (Promega), first-strand cDNA was synthesized from 2  $\mu$ g total RNA using the  
26  
27 iScript cDNA synthesis kit (Bio-Rad). Relative mRNA expression levels were  
28  
29 determined using an optimized two-step SYBR Green I real-time quantitative RT-PCR  
30  
31 assay with minor modifications (Vandesompele et al., 2002a). Primer sequences are  
32  
33 available in the public RTPrimerDB database (<http://medgen.ugent.be/rtprimerdb/>)  
34  
35 (Pattyn et al., 2003, 2006): *GAPDH* [RTPrimerDB ID 3], *SDHA* [7], *UBC* [8], *NEFH*  
36  
37 [3504], *NEFL* [3505], *NEFM* [3507], and *CHAT* [3502]. The PCR was run on a  
38  
39 LightCycler 480 instrument (Roche) in duplicate reactions of 7.5  $\mu$ L, containing 250 nM  
40  
41 of each primer and cDNA equivalent to 20 ng of total RNA. Gene expression levels and  
42  
43 PCR efficiency, along with its standard error, were calculated using qBasePlus 1.0  
44  
45 analysis software (<http://www.biogazelle.com>) (Hellemans et al., 2007), which employs a  
46  
47 delta-Ct relative quantification model with PCR efficiency correction and multiple  
48  
49  
50  
51  
52  
53  
54  
55  
56  
57  
58  
59  
60

1  
2  
3  
4  
5  
6  
7  
8  
9  
10  
11  
12  
13  
14  
15  
16  
17  
18  
19  
20  
21  
22  
23  
24  
25  
26  
27  
28  
29  
30  
31  
32  
33  
34  
35  
36  
37  
38  
39  
40  
41  
42  
43  
44  
45  
46  
47  
48  
49  
50  
51  
52  
53  
54  
55  
56  
57  
58  
59  
60

reference gene normalization (Vandesompele et al., 2002b). Expression levels of *GAPDH*,  
*SDHA* and *UBC* were used for normalization.

For Peer Review

## Results

### **Adenoviral transduction efficiency of neuroblastoma cells and expression of coxsackie-adenovirus receptors (CAR) on the cell surface**

To determine the infectivity of neuroblastoma cells by adenoviral vectors and the efficiency of transgene expression, cells were infected with a recombinant replication-defective adenovirus expressing GFP under control of the CMV promoter (Ad.CMV-*GFP*) at various MOIs (ranging from 12.5 to 200 pfu/cell) and monitored for the expression of GFP 24 h postinfection using flow cytometry. Transduction efficiency was assessed by calculating the percentage of cells expressing GFP. This analysis was performed on five human neuroblastoma cell lines [IMR-32, NGP, SHEP, SK-N-BE(2c), and SK-N-SH], on normal human melanocytes immortalized by SV40 T-antigen (FM-516-SV), and on human DU-145 prostate carcinoma cells. The immortalized melanocytes were chosen as a reference point in this study, as they share a common embryonic origin with neuroblastoma cells and as the exact normal counterparts for this malignancy, human fetal neuroblasts, are not available due to ethical and technical considerations. The DU-145 cells were included as a positive control, since these cells are characterized by a high level of surface expression of CAR proteins, which mediate adenovirus attachment and uptake in cells, and accordingly by an excellent adenoviral infectivity (Lebedeva et al., 2003). As shown in Figure 1, the adenoviral transduction efficiency of neuroblastoma cells was MOI-dependent and comparable to that obtained with the DU-145 prostate carcinoma cells. At an MOI of 200 pfu/cell, transduction efficiency ranged from 62% to 88% for neuroblastoma cells [percentage of cells positive for GFP expression: SK-N-

1  
2  
3 BE(2c), 62%; NGP, 63%; IMR-32, 66%; SK-N-SH, 86%; SHEP, 88%] and was 83% for  
4  
5  
6 DU-145 cells. A slightly lower transduction efficiency was recorded for FM-516-SV  
7  
8 immortalized melanocytes (55% of cells positive for GFP expression at 200 pfu/cell).  
9

10  
11  
12 We next investigated the expression of CAR on the cell surface by flow cytometry using  
13  
14 monoclonal antibodies against CAR (Table 1). Surface expression of this receptor was  
15  
16 detectable for all seven cell lines in this study, as evidenced by the Kolmogorov-Smirnov  
17  
18 two-sample test for analysis of flow cytometric histograms ( $P < .001$  for each cell line).  
19  
20 Analysis of the peak shift in fluorescence signal after staining with anti-CAR antibody  
21  
22 and FITC-conjugated secondary antibody indicated the following order of surface CAR  
23  
24 number and availability: DU-145 > IMR-32 > NGP > SHEP > SK-N-SH > SK-N-BE(2c)  
25  
26 > FM-516-SV. Based on these results, it is obvious that a simple correlative relationship  
27  
28 does not exist between surface CAR levels and GFP expression after exposure of cells to  
29  
30 Ad.CMV-*GFP*, suggesting a differential regulation of transgene expression after virus  
31  
32 entry.  
33  
34  
35  
36  
37  
38  
39  
40

41 Taken together, these data indicate that efficient adenoviral infection and transgene  
42  
43 expression is achievable in neuroblastoma cells, and support the development of  
44  
45 adenovirus-mediated gene therapy approaches for neuroblastoma.  
46  
47  
48  
49

50 **Expression of *hPNPase*<sup>old-35</sup> in FM-516-SV and neuroblastoma cells following**  
51  
52 **adenoviral gene transfer**  
53  
54  
55  
56  
57  
58  
59  
60



1  
2  
3 For assessment of the therapeutic potential of adenovirus-based *hPNPase*<sup>old-35</sup> delivery  
4  
5 for the treatment of neuroblastoma, we decided to explore both the effects of a classical  
6  
7 gene expression vector as well as of gene transfer under control of a promoter with  
8  
9 cancer-specific properties. Previous studies in multiple tumor models, including human  
10  
11 breast carcinoma, glioblastoma multiforme, pancreatic carcinoma and prostate cancer,  
12  
13 demonstrated a significantly higher activity of the *PEG-3* promoter in tumor cells  
14  
15 compared to their normal counterparts (Su et al., 2005; Chan et al., 2008). We  
16  
17 constructed two replication-incompetent adenoviruses, Ad.CMV-*hPNPase*<sup>old-35</sup> and  
18  
19 Ad.PEG-*hPNPase*<sup>old-35</sup>, in which *hPNPase*<sup>old-35</sup> expression is driven by the CMV minimal  
20  
21 promoter and by the minimal promoter region of *PEG-3*, respectively. The *hPNPase*<sup>old-35</sup>  
22  
23 transgene was engineered to encode a hemagglutinin (HA)-tag at the COOH-terminus for  
24  
25 monitoring expression. To determine the optimum MOI of Ad.CMV-*hPNPase*<sup>old-35</sup> and  
26  
27 Ad.PEG-*hPNPase*<sup>old-35</sup> infection, neuroblastoma and FM-516-SV cells were infected at  
28  
29 25, 50, 100 and 200 pfu/cell, and transgene expression was measured by Western blot  
30  
31 analysis using an anti-HA antibody. The empty adenoviral vector, Ad.*vec*, was used as a  
32  
33 control.  
34  
35  
36  
37  
38  
39  
40  
41  
42

43 As illustrated in Figure 2, infection with Ad.CMV-*hPNPase*<sup>old-35</sup> induced an MOI-  
44  
45 dependent expression of *hPNPase*<sup>old-35</sup> in both FM-516-SV immortalized melanocytes  
46  
47 and neuroblastoma cells. In contrast, infection with Ad.PEG-*hPNPase*<sup>old-35</sup> did not result  
48  
49 in *hPNPase*<sup>old-35</sup> expression in FM-516-SV cells, while the degree of transgene  
50  
51 expression in neuroblastoma cells after incubation with this adenovirus was variable,  
52  
53 ranging from weak HA bands in SHEP and SK-N-BE(2c) cells to a pronounced dose-  
54  
55  
56  
57  
58  
59  
60

1  
2  
3 dependent expression in IMR-32, NGP and SK-N-SH cells. These results validate the  
4  
5 functionality of both constructed *hPNPase<sup>old-35</sup>*-encoding adenoviral vectors and  
6  
7 demonstrate that the *PEG-3* promoter is capable of selectively targeting gene expression  
8  
9 in the majority of human neuroblastoma cells. We selected 100 pfu/cell as the optimal  
10  
11 working concentration for further experiments, as infection with Ad.CMV-*hPNPase<sup>old-35</sup>*  
12  
13 and Ad.PEG-*hPNPase<sup>old-35</sup>* at 200 pfu/cell resulted in markedly rapid cell death.  
14  
15  
16  
17

18  
19  
20 **Selective growth suppression by Ad.CMV-*hPNPase<sup>old-35</sup>* and Ad.PEG-*hPNPase<sup>old-35</sup>***  
21  
22 **in neuroblastoma cells**  
23

24 We next addressed whether adenovirus-mediated *hPNPase<sup>old-35</sup>* gene transfer could  
25  
26 selectively inhibit the growth of neuroblastoma cells. We therefore infected FM-516-SV  
27  
28 melanocytes and neuroblastoma cells with Ad.*vec*, Ad.CMV-*hPNPase<sup>old-35</sup>* and Ad.PEG-  
29  
30 *hPNPase<sup>old-35</sup>* at 100 pfu/cell, and monitored the number of viable cells by MTT assay at  
31  
32 1, 3 and 5 days postinfection. As depicted in Figure 3, infection with Ad.CMV-  
33  
34 *hPNPase<sup>old-35</sup>* and Ad.PEG-*hPNPase<sup>old-35</sup>* resulted in a pronounced suppression of growth  
35  
36 of IMR-32, NGP, SK-N-BE(2c) and SK-N-SH cells. These growth-inhibitory effects  
37  
38 became apparent from 3 days after infection, and were most prominent at day 5. It should  
39  
40 be noted that exposure to the empty adenoviral vector, Ad.*vec*, also resulted in some  
41  
42 growth inhibition of these cells, but this effect was considerably smaller than the decrease  
43  
44 in cell number induced by the *hPNPase<sup>old-35</sup>*-encoding adenoviruses [additional degree of  
45  
46 growth suppression due to the transgene component, relative to the number of Ad.*vec*-  
47  
48 infected cells, at day 5 postinfection: 50-60% for IMR-32, NGP and SK-N-SH cells, and  
49  
50 20-30% for SK-N-BE(2c) cells]. On the contrary, transduction of SHEP neuroblastoma  
51  
52  
53  
54  
55  
56  
57  
58  
59  
60

1  
2  
3 cells and FM-516-SV melanocytes with Ad.CMV-*hPNPase*<sup>old-35</sup> and Ad.PEG-  
4  
5 *hPNPase*<sup>old-35</sup> resulted in only a slight decrease in the number of viable cells at day 5  
6  
7  
8 postinfection.  
9

10  
11  
12 Taken together, these findings suggest that both Ad.CMV-*hPNPase*<sup>old-35</sup> and Ad.PEG-  
13  
14 *hPNPase*<sup>old-35</sup> have the ability to suppress the growth of most human neuroblastoma cells.  
15  
16 The observation that infection with Ad.CMV-*hPNPase*<sup>old-35</sup> exerted only a limited  
17  
18 growth-inhibitory effect on FM-516-SV immortalized normal melanocytes, despite a  
19  
20 distinct induction of *hPNPase*<sup>old-35</sup> expression, supports the notion of *hPNPase*<sup>old-35</sup> as a  
21  
22 tumor-selective growth-suppressive gene and hence as a valuable gene therapy tool for  
23  
24 the treatment of cancer.  
25  
26  
27  
28  
29  
30  
31

### 32 **Effects of adenoviral infection and *hPNPase*<sup>old-35</sup> expression on cell cycle progression,** 33 34 **apoptosis, and neuronal differentiation of neuroblastoma cells**

35  
36 To investigate the mechanism of growth inhibition, cellular effects of adenovirus-  
37  
38 mediated *hPNPase*<sup>old-35</sup> expression were studied in detail in two well-responsive  
39  
40 neuroblastoma cell types, NGP and SK-N-SH, and in the poorly responsive SHEP cells.  
41  
42 Flow cytometric cell cycle profiling of NGP cells indicated that infection with Ad.CMV-  
43  
44 *hPNPase*<sup>old-35</sup> and Ad.PEG-*hPNPase*<sup>old-35</sup> at 100 pfu/cell resulted in a decrease of cells in  
45  
46 the S phase, reflective of inhibition of DNA synthesis (Fig. 4A). At early timepoints after  
47  
48 infection, this change was mainly accompanied by accumulation of NGP cells in the G<sub>1</sub>  
49  
50 phase, while a gradual increase in the sub-G<sub>1</sub> (A<sub>0</sub>) population of cells at day 4 and 5  
51  
52 postinfection indicated the occurrence of apoptotic cell death. Infection of NGP cells with  
53  
54  
55  
56  
57  
58  
59  
60

1  
2  
3 Ad.*vec* at 100 pfu/cell induced a comparable G<sub>1</sub> cell cycle arrest, but only a mild degree  
4 of apoptosis. The response of SK-N-SH cells to adenovirus-mediated *hPNPase*<sup>old-35</sup> gene  
5 transfer was characterized by a more extensive and more rapid induction of apoptosis, as  
6 evidenced by the A<sub>0</sub> fraction, with an initial arrest at the G<sub>1</sub>/S boundary still observable  
7 after Ad.PEG-*hPNPase*<sup>old-35</sup> infection (Fig. 4B). The empty adenoviral vector, Ad.*vec*,  
8 also elicited an inhibition of the G<sub>1</sub>/S transition in SK-N-SH cells, but only a modest  
9 increase in hypodiploid DNA content. In contrast to the pronounced degree of apoptosis  
10 observed in NGP and SK-N-SH cells following Ad.CMV-*hPNPase*<sup>old-35</sup> and Ad.PEG-  
11 *hPNPase*<sup>old-35</sup> infection, transduction of SHEP cells with these viruses resulted in only a  
12 limited increase in the A<sub>0</sub> population, along with a slight G<sub>1</sub> arrest (Fig. 4C).  
13  
14  
15  
16  
17  
18  
19  
20  
21  
22  
23  
24  
25  
26  
27  
28

29 The induction of apoptosis by Ad.CMV-*hPNPase*<sup>old-35</sup> and Ad.PEG-*hPNPase*<sup>old-35</sup>  
30 infection of NGP and SK-N-SH cells was confirmed by analysis of caspase-3 and  
31 caspase-7 activity (Fig. 5). Adenovirus-mediated *hPNPase*<sup>old-35</sup> expression evoked a 2- to  
32 3-fold and a 3- to 5-fold increase in caspase-3 and caspase-7 activity in NGP and SK-N-  
33 SH cells, respectively, measured 2-3 days after infection at 100 pfu/cell. No activation of  
34 these apoptotic effector enzymes was recorded in Ad.*vec*-infected NGP and SK-N-SH  
35 cells. Exposure of SHEP cells to Ad.CMV-*hPNPase*<sup>old-35</sup> and Ad.PEG-*hPNPase*<sup>old-35</sup> at  
36 100 pfu/cell did not induce caspase-3 and caspase-7 activity, in keeping with the limited  
37 growth-suppressive effects that were observed using MTT assays.  
38  
39  
40  
41  
42  
43  
44  
45  
46  
47  
48  
49  
50  
51  
52

53 Interestingly, microscopic evaluation of adenovirally infected NGP cells revealed striking  
54 morphological changes indicative of neuronal differentiation, such as the acquisition of a  
55  
56  
57  
58  
59  
60

1  
2  
3 bipolar or stellate appearance, and the formation of long neurites with varicosities and  
4 growth cone-like endings (Fig. 6A). These alterations were observed after infection of  
5 NGP cells with either of the evaluated adenoviruses (*Ad.vec*, *Ad.CMV-hPNPase<sup>old-35</sup>*,  
6 and *Ad.PEG-hPNPase<sup>old-35</sup>*), but not after transduction of any other cell type in this study.  
7  
8 Confirmation of the neuronal differentiation process following adenoviral infection of  
9 NGP cells was obtained by expression analysis of neuronal differentiation markers using  
10 real-time quantitative RT-PCR (Fig. 6B). Adenoviral infection of NGP cells resulted in a  
11 marked increase in expression of the genes encoding the heavy, light, and medium  
12 neurofilament subunits (*NEFH*, *NEFL*, and *NEFM*, respectively) and of the rate-limiting  
13 enzyme in the biosynthesis of acetylcholine (*CHAT*), suggestive of differentiation along a  
14 cholinergic neuronal lineage.  
15  
16  
17  
18  
19  
20  
21  
22  
23  
24  
25  
26  
27  
28  
29  
30  
31

32 Collectively, these data demonstrate that adenoviral infection of neuroblastoma cells  
33 results in a G<sub>1</sub> cell cycle arrest, which was accompanied by neuronal differentiation in  
34 NGP cells, that *hPNPase<sup>old-35</sup>* expression triggers a pronounced apoptotic response in  
35 NGP and SK-N-SH cells, and that the limited growth-inhibitory activity of *hPNPase<sup>old-35</sup>*  
36 gene delivery in SHEP cells correlates with a lack of apoptosis induction.  
37  
38  
39  
40  
41  
42  
43  
44  
45  
46  
47  
48  
49  
50  
51  
52  
53  
54  
55  
56  
57  
58  
59  
60

## Discussion

The poor survival rates of high-risk neuroblastoma patients and the long-term severe side effects of current treatment regimens clearly warrant development of more effective and less toxic therapeutic modalities. Gene therapy holds great promise to improve the treatment of cancer, as gene transfer offers in principle the most direct and rational means to counteract the multiplicity of genetic events underlying the neoplastic process or to bring about destruction or incapacitation of tumor cells. Efforts to develop gene therapeutic approaches for treatment of neuroblastoma have been relatively limited to date. The present study was undertaken to evaluate a promising growth-inhibitory gene, *hPNPase<sup>old-35</sup>*, operative through a mechanism completely different from those of conventional chemotherapeutic drugs, as a potential therapeutic agent for neuroblastoma, using adenovirus-mediated gene delivery with transgene expression driven by either the CMV promoter or by a cancer-selective promoter derived from the *PEG-3* gene. Our findings support the concept that *hPNPase<sup>old-35</sup>* is a negative regulator of growth and survival of neuroblastoma cells and that this gene may be exploited for an adenovirus-based gene therapy approach of neuroblastoma.

A prerequisite for a successful therapeutic modality is selective activity in tumor cells with minimal damage to normal cells. FM-516-SV immortalized normal melanocytes, which are, similarly to neuroblastoma cells, embryonically derived from the neural crest, were only to a limited extent suppressed in their growth after infection with Ad.CMV-*hPNPase<sup>old-35</sup>*, despite a clear induction of *hPNPase<sup>old-35</sup>* expression. In contrast, most

1  
2  
3 neuroblastoma cell types showed pronounced growth inhibition after transduction with  
4 Ad.CMV-*hPNPase*<sup>old-35</sup>. As selective delivery of genes to cancer cells remains one of the  
5  
6 major hurdles to clinical implementation of gene therapy approaches, we decided to  
7  
8 combine the growth-inhibitory effect of *hPNPase*<sup>old-35</sup> with the wide-ranging cancer-  
9  
10 selective activity of the *PEG-3* promoter (Su et al., 2005). Use of the latter promoter  
11  
12 induced a marked dose-dependent expression of *hPNPase*<sup>old-35</sup> and a profound growth  
13  
14 suppression in IMR-32, NGP and SK-N-SH neuroblastoma cells, suggesting eligibility of  
15  
16 a substantial fraction of neuroblastoma cases for treatment with *PEG-3* promoter-based  
17  
18 gene therapy regimens.  
19  
20  
21  
22  
23  
24  
25  
26

27 The precise mechanism of the cancer selectivity and resulting favorable therapeutic index  
28  
29 of the various antitumor ribonucleases described thus far remains to be elucidated (Benito  
30  
31 et al., 2005; Arnold and Ulbrich-Hofmann, 2006). With regard to *hPNPase*<sup>old-35</sup>, we  
32  
33 previously documented its ability to selectively degrade *c-myc* mRNA as essential to the  
34  
35 growth arrest induced by Ad.CMV-*hPNPase*<sup>old-35</sup> infection or IFN- $\beta$  treatment of  
36  
37 melanoma cells (Sarkar et al., 2003, 2006). We therefore investigated whether  
38  
39 *hPNPase*<sup>old-35</sup> was also capable of specifically degrading *N-myc* mRNA in neuroblastoma  
40  
41 cells, but this appears not to be the case (data not shown) and this would not have  
42  
43 explained the excellent growth-inhibitory and proapoptotic activity of adenovirus-  
44  
45 mediated *hPNPase*<sup>old-35</sup> gene transfer against the *N-myc* single-copy SK-N-SH cells. It is  
46  
47 possible that a preferential degradation of other mRNA species encoding key proteins in  
48  
49 neuroblastoma cell maintenance underlies the cytotoxic effect of *hPNPase*<sup>old-35</sup> on  
50  
51 neuroblastoma cells. Additional research to unravel determinants of the substrate  
52  
53  
54  
55  
56  
57  
58  
59  
60

1  
2  
3 specificity of *hPNPase*<sup>old-35</sup> activity will be needed to clarify this issue. Alternatively, it  
4  
5 might be that malignant neuroblastoma cells are more dependent than normal cells on the  
6  
7 overall integrity of their RNA due to their high proliferative and metabolic rate or due to  
8  
9 collateral proapoptotic signals derived from the myriad of stresses to which tumor cells  
10  
11 are subjected. Another explanation for the observed tumor selectivity of *hPNPase*<sup>old-35</sup>  
12  
13 relates to the possibility of degradation of microRNAs (miRNAs), as has been postulated  
14  
15 previously for other cytotoxic ribonucleases (Ardelt et al., 2003), since cumulating  
16  
17 evidence indicates that miRNAs are deeply implicated in tumor biology but of  
18  
19 considerably less importance in fully-developed normal cells.  
20  
21  
22  
23  
24  
25  
26

27 A more thorough understanding of the molecular mode of action of *hPNPase*<sup>old-35</sup> might  
28  
29 also shed light on the relatively resistant phenotype of SHEP cells. It is worth noting that  
30  
31 these cells also have a poor response to irradiation (Jasty et al., 1998; Tweddle et al.,  
32  
33 2001) and to various cytotoxic agents (unpublished observations), pointing at a more  
34  
35 general insensitivity of SHEP cells to certain cell death-inducing triggers. This might for  
36  
37 instance be related to a yet undefined block on apoptotic effector pathways in SHEP cells  
38  
39 (Jasty et al., 1998), but an alternative hypothesis involves the poor tumorigenicity of  
40  
41 these cells. SHEP cells, although widely used in neuroblastoma research, do neither form  
42  
43 colonies in soft agar nor tumors when injected in nude mice (Ross and Spengler, 2007),  
44  
45 and hence it can be questioned whether these tumor-derived cells still represent true  
46  
47 malignant cells. In such a scenario, it is not surprising that the response of SHEP cells to  
48  
49 adenovirus-mediated *hPNPase*<sup>old-35</sup> gene transfer resembles more closely the slight  
50  
51  
52  
53  
54  
55  
56  
57  
58  
59  
60



1  
2  
3 growth suppression induced in FM-516-SV immortalized normal melanocytes than the  
4  
5 strong apoptotic response of highly malignant neuroblastoma cells.  
6  
7

8  
9  
10 Interestingly, the process of adenoviral infection was sufficient to induce neuronal  
11  
12 differentiation of NGP cells. Neuroblastoma is thought to arise from precursor cells of the  
13  
14 sympathoadrenal system that are arrested at a developmental stage prior to completion of  
15  
16 lineage maturation (McConville and Forsyth, 2003). As such, it is not unexpected that the  
17  
18 induction of cell cycle arrest by adenoviral infection, which was observed in all cell lines  
19  
20 evaluated, might be coupled with resumption of execution of the differentiation program.  
21  
22 The observation of adenovirus-induced neuronal differentiation of NGP cells is however  
23  
24 of interest from a clinical perspective, as it opens the possibility that some neuroblastoma  
25  
26 tumors may mature after treatment with an adenovirus-based gene therapy approach.  
27  
28  
29  
30  
31

32  
33  
34 In summary, our results indicate that *hPNPase*<sup>old-35</sup> may have utility for gene-based  
35  
36 therapy of neuroblastoma and that the *PEG-3* promoter may provide a valuable tool for  
37  
38 selective gene delivery to most neuroblastoma cells. Further studies in experimental  
39  
40 animal models of neuroblastoma are essential to successfully translate this approach into  
41  
42 a viable therapeutic strategy for neuroblastoma.  
43  
44  
45  
46  
47  
48  
49  
50  
51  
52  
53  
54  
55  
56  
57  
58  
59  
60

## Acknowledgments

The present study was supported in part by National Institutes of Health grants P01 CA104177, R01 CA035675 and R01 CA102321, and the Samuel Waxman Cancer Research Foundation. T.V.M. is a research assistant from the Research Foundation – Flanders (FWO) and was supported by an FWO travel grant for this work. D.S. is the Harrison Endowed Scholar in Cancer Research. P.B.F. holds the Thelma Newmeyer Corman Chair in Cancer Research. W.A.W. and P.B.F. are Samuel Waxman Cancer Research Foundation Investigators. We thank Eun-Sook Park for adenovirus production and Justine Nuytens for assistance with real-time quantitative RT-PCR.

**Literature Cited**

- 1  
2  
3  
4  
5  
6  
7  
8 Ardelt B, Ardelt W, Darzynkiewicz Z. 2003. Cytotoxic ribonucleases and RNA  
9 interference (RNAi). *Cell Cycle* 2(1):22-24.  
10  
11  
12 Arnold U, Ulbrich-Hofmann R. 2006. Natural and engineered ribonucleases as potential  
13 cancer therapeutics. *Biotechnol Lett* 28(20):1615-1622.  
14  
15  
16  
17 Beck AK, Pass HI, Carbone M, Yang H. 2008. Ranpirnase as a potential antitumor  
18 ribonuclease treatment for mesothelioma and other malignancies. *Future Oncol*  
19  
20 4(3):341-349.  
21  
22  
23  
24 Benito A, Ribo M, Vilanova M. 2005. On the track of antitumour ribonucleases. *Mol*  
25  
26 *Biosyst* 1(4):294-302.  
27  
28  
29 Brodeur GM. 2003. Neuroblastoma: biological insights into a clinical enigma. *Nat Rev*  
30  
31 *Cancer* 3(3):203-216.  
32  
33  
34 Chan I, Lebedeva IV, Su ZZ, Sarkar D, Valerie K, Fisher PB. 2008. Progression elevated  
35 gene-3 promoter (PEG-Prom) confers cancer cell selectivity to human  
36 polynucleotide phosphorylase (*hPNPase<sup>old-35</sup>*)-mediated growth suppression. *J*  
37  
38 *Cell Physiol* 215(2):401-409.  
39  
40  
41  
42  
43 Cinatl J, Jr., Cinatl J, Kotchetkov R, Matousek J, Woodcock BG, Koehl U, Vogel JU,  
44  
45 Kornhuber B, Schwabe D. 2000. Bovine seminal ribonuclease exerts selective  
46 cytotoxicity toward neuroblastoma cells both sensitive and resistant to  
47  
48  
49  
50  
51  
52  
53  
54 Cinatl J, Jr., Cinatl J, Kotchetkov R, Vogel JU, Woodcock BG, Matousek J, Pouckova P,  
55  
56  
57  
58  
59  
60 Kornhuber B. 1999. Bovine seminal ribonuclease selectively kills human

- 1  
2  
3 multidrug-resistant neuroblastoma cells via induction of apoptosis. *Int J Oncol*  
4  
5 15(5):1001-1009.  
6  
7  
8 D'Alessio G. 1993. New and cryptic biological messages from RNases. *Trends Cell Biol*  
9  
10 3(4):106-109.  
11  
12 Hellemans J, Mortier G, De Paepe A, Speleman F, Vandesompele J. 2007. qBase relative  
13  
14 quantification framework and software for management and automated analysis  
15  
16 of real-time quantitative PCR data. *Genome Biol* 8(2):R19.  
17  
18  
19 Holmes M, Rosenberg E, Valerie K. 2003. Adenovirus expressing p53. *Methods Mol*  
20  
21 Biol 234:1-16.  
22  
23  
24 Jasty R, Lu J, Irwin T, Suchard S, Clarke MF, Castle VP. 1998. Role of p53 in the  
25  
26 regulation of irradiation-induced apoptosis in neuroblastoma cells. *Mol Genet*  
27  
28 *Metab* 65(2):155-164.  
29  
30  
31 Kotchetkov R, Cinatl J, Matousek J, Vogel J, Pouckova P, Wagner M, Kornhuber B,  
32  
33 Schwabe D, Cinatl J, Jr. 2000. Bovine seminal ribonuclease inhibits in vivo  
34  
35 growth of human neuroblastoma cells. *Oncol Rep* 7(2):363-367.  
36  
37  
38 Lebedeva IV, Sarkar D, Su ZZ, Kitada S, Dent P, Stein CA, Reed JC, Fisher PB. 2003.  
39  
40 Bcl-2 and Bcl-x<sub>L</sub> differentially protect human prostate cancer cells from induction  
41  
42 of apoptosis by melanoma differentiation associated gene-7, *mda-7/IL-24*.  
43  
44 *Oncogene* 22(54):8758-8773.  
45  
46  
47 Lebedeva IV, Su ZZ, Chang Y, Kitada S, Reed JC, Fisher PB. 2002. The cancer growth  
48  
49 suppressing gene *mda-7* induces apoptosis selectively in human melanoma cells.  
50  
51 *Oncogene* 21(5):708-718.  
52  
53  
54  
55  
56  
57  
58  
59  
60

- 1  
2  
3 Leszczyniecka M, Kang DC, Sarkar D, Su ZZ, Holmes M, Valerie K, Fisher PB. 2002.  
4  
5 Identification and cloning of human polynucleotide phosphorylase, *hPNPase*<sup>old-35</sup>,  
6  
7 in the context of terminal differentiation and cellular senescence. Proc Natl Acad  
8  
9 Sci U S A 99(26):16636-16641.  
10  
11  
12 Leszczyniecka M, Su ZZ, Kang DC, Sarkar D, Fisher PB. 2003. Expression regulation  
13  
14 and genomic organization of human polynucleotide phosphorylase, *hPNPase*<sup>old-35</sup>,  
15  
16 a Type I interferon inducible early response gene. Gene 316:143-156.  
17  
18  
19 Maris JM, Hogarty MD, Bagatell R, Cohn SL. 2007. Neuroblastoma. Lancet  
20  
21 369(9579):2106-2120.  
22  
23  
24 McConville CM, Forsyth J. 2003. Neuroblastoma – a developmental perspective. Cancer  
25  
26 Lett 197(1-2):3-9.  
27  
28  
29 Michaelis M, Cinatl J, Anand P, Rothweiler F, Kotchetkov R, Deimling A, Doerr HW,  
30  
31 Shogen K, Cinatl J, Jr. 2007. Onconase induces caspase-independent cell death in  
32  
33 chemoresistant neuroblastoma cells. Cancer Lett 250(1):107-116.  
34  
35  
36 Pattyn F, Robbrecht P, De Paepe A, Speleman F, Vandesompele J. 2006. RTPrimerDB:  
37  
38 the real-time PCR primer and probe database, major update 2006. Nucleic Acids  
39  
40 Res 34(Database issue):D684-688.  
41  
42  
43 Pattyn F, Speleman F, De Paepe A, Vandesompele J. 2003. RTPrimerDB: the real-time  
44  
45 PCR primer and probe database. Nucleic Acids Res 31(1):122-123.  
46  
47  
48 Ross RA, Spengler BA. 2007. Human neuroblastoma stem cells. Semin Cancer Biol  
49  
50 17(3):241-247.  
51  
52  
53 Sarkar D, Fisher PB. 2006. Polynucleotide phosphorylase: an evolutionary conserved  
54  
55 gene with an expanding repertoire of functions. Pharmacol Ther 112(1):243-263.  
56  
57  
58  
59  
60

- 1  
2  
3 Sarkar D, Lebedeva IV, Emdad L, Kang DC, Baldwin AS, Jr., Fisher PB. 2004. Human  
4 polynucleotide phosphorylase (*hPNPase<sup>old-35</sup>*): a potential link between aging and  
5 inflammation. *Cancer Res* 64(20):7473-7478.  
6  
7  
8  
9  
10 Sarkar D, Leszczyniecka M, Kang DC, Lebedeva IV, Valerie K, Dhar S, Pandita TK,  
11 Fisher PB. 2003. Down-regulation of Myc as a potential target for growth arrest  
12 induced by human polynucleotide phosphorylase (*hPNPase<sup>old-35</sup>*) in human  
13 melanoma cells. *J Biol Chem* 278(27):24542-24551.  
14  
15  
16  
17  
18  
19 Sarkar D, Park ES, Barber GN, Fisher PB. 2007. Activation of double-stranded RNA-  
20 dependent protein kinase, a new pathway by which human polynucleotide  
21 phosphorylase (*hPNPase<sup>old-35</sup>*) induces apoptosis. *Cancer Res* 67(17):7948-7953.  
22  
23  
24  
25  
26  
27 Sarkar D, Park ES, Emdad L, Randolph A, Valerie K, Fisher PB. 2005. Defining the  
28 domains of human polynucleotide phosphorylase (*hPNPase<sup>OLD-35</sup>*) mediating  
29 cellular senescence. *Mol Cell Biol* 25(16):7333-7343.  
30  
31  
32  
33  
34 Sarkar D, Park ES, Fisher PB. 2006. Defining the mechanism by which IFN- $\beta$   
35 downregulates *c-myc* expression in human melanoma cells: pivotal role for human  
36 polynucleotide phosphorylase (*hPNPase<sup>old-35</sup>*). *Cell Death Differ* 13(9):1541-1553.  
37  
38  
39  
40  
41 Su ZZ, Sarkar D, Emdad L, Duigou GJ, Young CS, Ware J, Randolph A, Valerie K,  
42 Fisher PB. 2005. Targeting gene expression selectively in cancer cells by using  
43 the progression-elevated gene-3 promoter. *Proc Natl Acad Sci U S A*  
44 102(4):1059-1064.  
45  
46  
47  
48  
49  
50  
51 Tweddle DA, Malcolm AJ, Cole M, Pearson AD, Lunec J. 2001. p53 cellular localization  
52 and function in neuroblastoma: evidence for defective G<sub>1</sub> arrest despite WAF1  
53 induction in MYCN-amplified cells. *Am J Pathol* 158(6):2067-2077.  
54  
55  
56  
57  
58  
59  
60

- 1  
2  
3 Van Maerken T, Speleman F, Vermeulen J, Lambertz I, De Clercq S, De Smet E, Yigit N,  
4  
5 Coppins V, Philippe J, De Paepe A, Marine JC, Vandesomepele J. 2006. Small-  
6  
7 molecule MDM2 antagonists as a new therapy concept for neuroblastoma. *Cancer*  
8  
9 *Res* 66(19):9646-9655.  
10  
11  
12 Vandesomepele J, De Paepe A, Speleman F. 2002a. Elimination of primer-dimer artifacts  
13  
14 and genomic coamplification using a two-step SYBR green I real-time RT-PCR.  
15  
16 *Anal Biochem* 303(1):95-98.  
17  
18  
19 Vandesomepele J, De Preter K, Pattyn F, Poppe B, Van Roy N, De Paepe A, Speleman F.  
20  
21 2002b. Accurate normalization of real-time quantitative RT-PCR data by  
22  
23 geometric averaging of multiple internal control genes. *Genome Biol*  
24  
25 3(7):RESEARCH0034.  
26  
27  
28 Vasandani VM, Burris JA, Sung C. 1999. Reversible nephrotoxicity of onconase and  
29  
30 effect of lysine pH on renal onconase uptake. *Cancer Chemother Pharmacol*  
31  
32 44(2):164-169.  
33  
34  
35 Vasandani VM, Wu YN, Mikulski SM, Youle RJ, Sung C. 1996. Molecular determinants  
36  
37 in the plasma clearance and tissue distribution of ribonucleases of the  
38  
39 ribonuclease A superfamily. *Cancer Res* 56(18):4180-4186.  
40  
41  
42 Youle RJ, Newton D, Wu YN, Gadina M, Rybak SM. 1993. Cytotoxic ribonucleases and  
43  
44 chimeras in cancer therapy. *Crit Rev Ther Drug Carrier Syst* 10(1):1-28.  
45  
46  
47 Young IT. 1977. Proof without prejudice: use of the Kolmogorov-Smirnov test for the  
48  
49 analysis of histograms from flow systems and other sources. *J Histochem*  
50  
51 *Cytochem* 25(7):935-941.  
52  
53  
54  
55  
56  
57  
58  
59  
60

## Figure legends

**Figure 1.** Infection with Ad.CMV-*GFP* induces GFP expression in neuroblastoma cells.

A panel of five human neuroblastoma cell lines [IMR-32, NGP, SHEP, SK-N-BE(2c), and SK-N-SH], DU-145 human prostate carcinoma cells, and FM-516-SV immortalized human melanocytes were infected with Ad.CMV-*GFP* at the indicated MOIs, and analyzed for the expression of GFP 24 h postinfection using flow cytometry. Columns represent the mean percentages of GFP-positive cells of three different experiments, and error bars indicate standard errors of the mean. Asterisk, percentage of GFP-positive cells 24 h after mock infection ranged from 0.19% to 0.22% for all cell lines.

**Figure 2.** Expression of *hPNPase*<sup>old-35</sup> in FM-516-SV human melanocytes and neuroblastoma cells following adenoviral gene transfer. FM-516-SV immortalized melanocytes and a panel of five neuroblastoma cell lines were infected with Ad.*vec*, Ad.CMV-*hPNPase* (Ad.CMV-*hPNPase*<sup>old-35</sup>; hemagglutinin [HA]-tagged *hPNPase*<sup>old-35</sup> expression driven by the CMV promoter), or Ad.PEG-*hPNPase* (Ad.PEG-*hPNPase*<sup>old-35</sup>; HA-tagged *hPNPase*<sup>old-35</sup> expression driven by the *PEG-3* promoter) at the indicated MOIs, and probed 48 h postinfection for *hPNPase*<sup>old-35</sup> expression by Western blot analysis using an anti-HA antibody. Expression of EF1 $\alpha$  is shown as loading control.

**Figure 3.** Effect of Ad.*vec*, Ad.CMV-*hPNPase*<sup>old-35</sup>, and Ad.PEG-*hPNPase*<sup>old-35</sup> on growth and viability of FM-516-SV human melanocytes and neuroblastoma cells. Exponentially growing cells were untreated or infected with Ad.*vec*, Ad.CMV-*hPNPase*



1  
2  
3 (Ad.CMV-*hPNPase*<sup>old-35</sup>), or Ad.PEG-*hPNPase* (Ad.PEG-*hPNPase*<sup>old-35</sup>) at 100 pfu/cell,  
4  
5 and the number of viable cells was determined at 1, 3 and 5 days postinfection using  
6  
7 MTT assay. Points represent the mean relative numbers of viable cells of three  
8  
9 independent experiments, and error bars indicate standard errors of the mean.  
10  
11

12  
13  
14  
15 **Figure 4.** Effect of Ad.*vec*, Ad.CMV-*hPNPase*<sup>old-35</sup>, and Ad.PEG-*hPNPase*<sup>old-35</sup> on cell  
16  
17 cycle distribution and hypodiploid DNA content of human neuroblastoma cells. NGP (A),  
18  
19 SK-N-SH (B), and SHEP (C) cells were untreated or infected with Ad.*vec*, Ad.CMV-  
20  
21 *hPNPase* (Ad.CMV-*hPNPase*<sup>old-35</sup>), or Ad.PEG-*hPNPase* (Ad.PEG-*hPNPase*<sup>old-35</sup>) at 100  
22  
23 pfu/cell, harvested at 2, 3, 4 and 5 days postinfection, and monitored for DNA content by  
24  
25 propidium iodide staining and flow cytometric analysis. Columns represent the mean cell  
26  
27 cycle and apoptotic fractions of three different experiments, and error bars correspond to  
28  
29 standard errors of the mean.  
30  
31  
32

33  
34  
35  
36 **Figure 5.** Effect of Ad.*vec*, Ad.CMV-*hPNPase*<sup>old-35</sup>, and Ad.PEG-*hPNPase*<sup>old-35</sup> on  
37  
38 caspase-3 and caspase-7 activity in human neuroblastoma cells. NGP, SK-N-SH, and  
39  
40 SHEP cells were untreated or infected with Ad.*vec*, Ad.CMV-*hPNPase* (Ad.CMV-  
41  
42 *hPNPase*<sup>old-35</sup>), or Ad.PEG-*hPNPase* (Ad.PEG-*hPNPase*<sup>old-35</sup>) at 100 pfu/cell, and the  
43  
44 combined activity of caspase-3 and caspase-7, relative to uninfected cells, was  
45  
46 determined at 2 and 3 days postinfection. Columns represent the mean caspase-3 and  
47  
48 caspase-7 activity values of triplicate wells, and error bars correspond to standard  
49  
50 deviations.  
51  
52  
53  
54  
55  
56  
57  
58  
59  
60

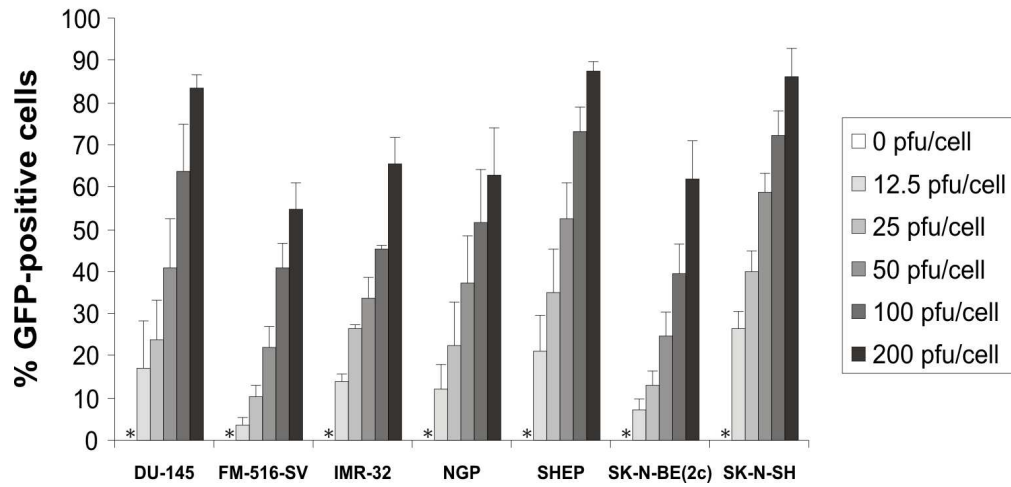
1  
2  
3 **Figure 6.** Adenoviral infection induces neuronal differentiation of NGP human  
4 neuroblastoma cells. A: Phase-contrast images of NGP cells left untreated for five days  
5 (*left*) and five days after infection with *Ad.vec* (*right*). Adenoviral infection induced clear  
6 morphological signs of neuronal differentiation, including a polar morphology and  
7 extensive outgrowth of neuritic processes, which formed a netlike arrangement. Similar  
8 morphological changes were observed after infection of NGP cells with *Ad.CMV-*  
9 *hPNPase<sup>old-35</sup>* or *Ad.PEG-hPNPase<sup>old-35</sup>* (not shown). B: Real-time quantitative RT-PCR  
10 analysis of expression of neuronal differentiation markers (*NEFH*, *NEFL*, *NEFM*, and  
11 *CHAT*) in NGP cells harvested five days after exposure to control conditions or to  
12 infection with *Ad.vec*, *Ad.CMV-hPNPase* (*Ad.CMV-hPNPase<sup>old-35</sup>*), or *Ad.PEG-*  
13 *hPNPase* (*Ad.PEG-hPNPase<sup>old-35</sup>*) at 100 pfu/cell. Columns represent the mean mRNA  
14 expression levels derived from two RT-PCR measurements, and error bars indicate  
15 standard deviations.  
16  
17  
18  
19  
20  
21  
22  
23  
24  
25  
26  
27  
28  
29  
30  
31  
32  
33  
34  
35  
36  
37  
38  
39  
40  
41  
42  
43  
44  
45  
46  
47  
48  
49  
50  
51  
52  
53  
54  
55  
56  
57  
58  
59  
60

**Table 1.** Expression of coxsackie-adenovirus receptors (CAR) on the surface of DU-145 prostate carcinoma cells, FM-516-SV immortalized melanocytes, and neuroblastoma cells

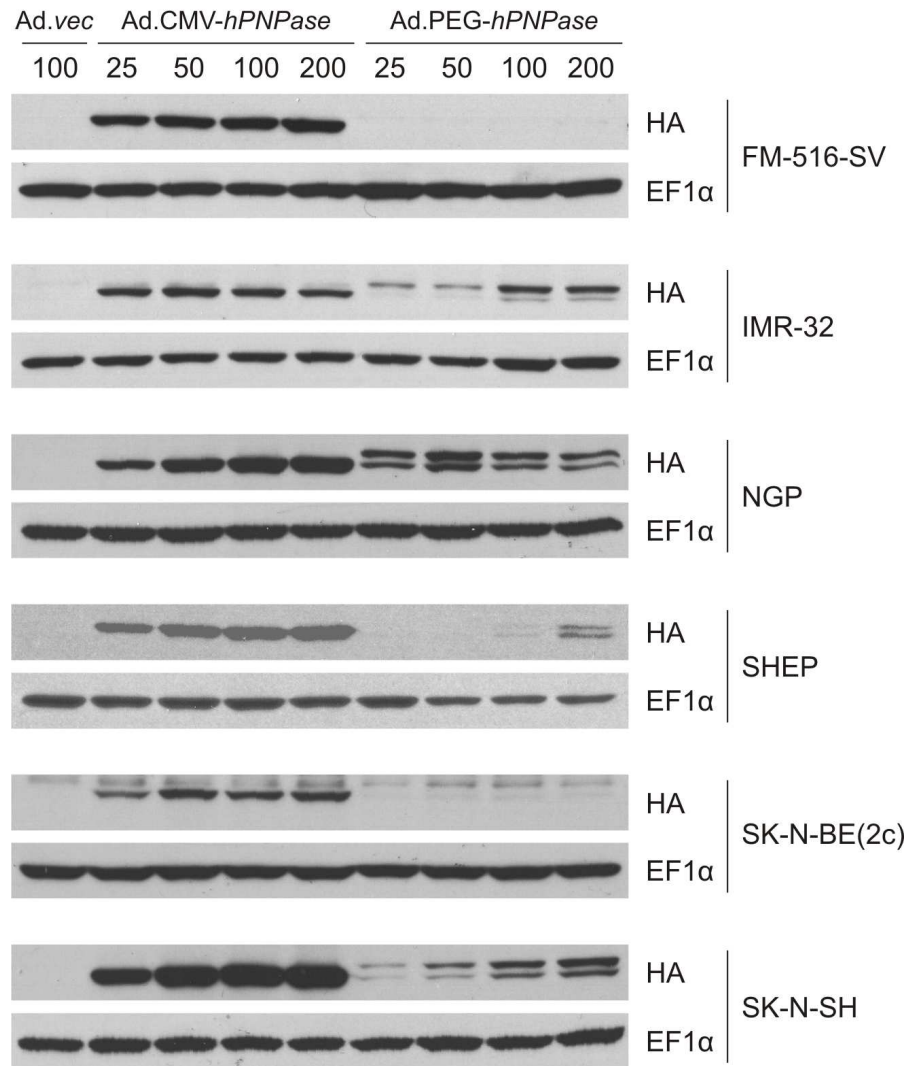
	DU-145	FM-516-SV	IMR-32	NGP	SHEP	SK-N-BE(2c)	SK-N-SH
<i>D</i> value	0.88	0.42	0.68	0.79	0.53	0.33	0.54
Peak shift	4.66	0.61	1.72	1.34	1.30	0.74	1.23

Cells were incubated with mouse monoclonal anti-CAR antibody, washed, stained with FITC-labeled anti-mouse immunoglobulins, washed, analyzed by flow cytometry, and compared with a number of appropriate controls, as described in Material and Methods. The *D* value, calculated by the Kolmogorov-Smirnov two-sample test for analysis of flow cytometric histograms and reflecting the greatest difference between the cumulative distribution functions derived from the histograms (Young, 1977), indicated for all cell types in this study the presence of CAR surface expression at the 99.9% confidence level. The peak shift, computed as a ratio  $(P_{CAR} - P_{ctrl})/P_{ctrl}$  with  $P_{CAR}$  and  $P_{ctrl}$  being the median of the fluorescent peak of the flow cytometric histogram of the CAR-stained cells and of the control cells with the highest FITC signal intensity, respectively, allows for comparison of surface CAR number and availability between different cell types.

Peer Review

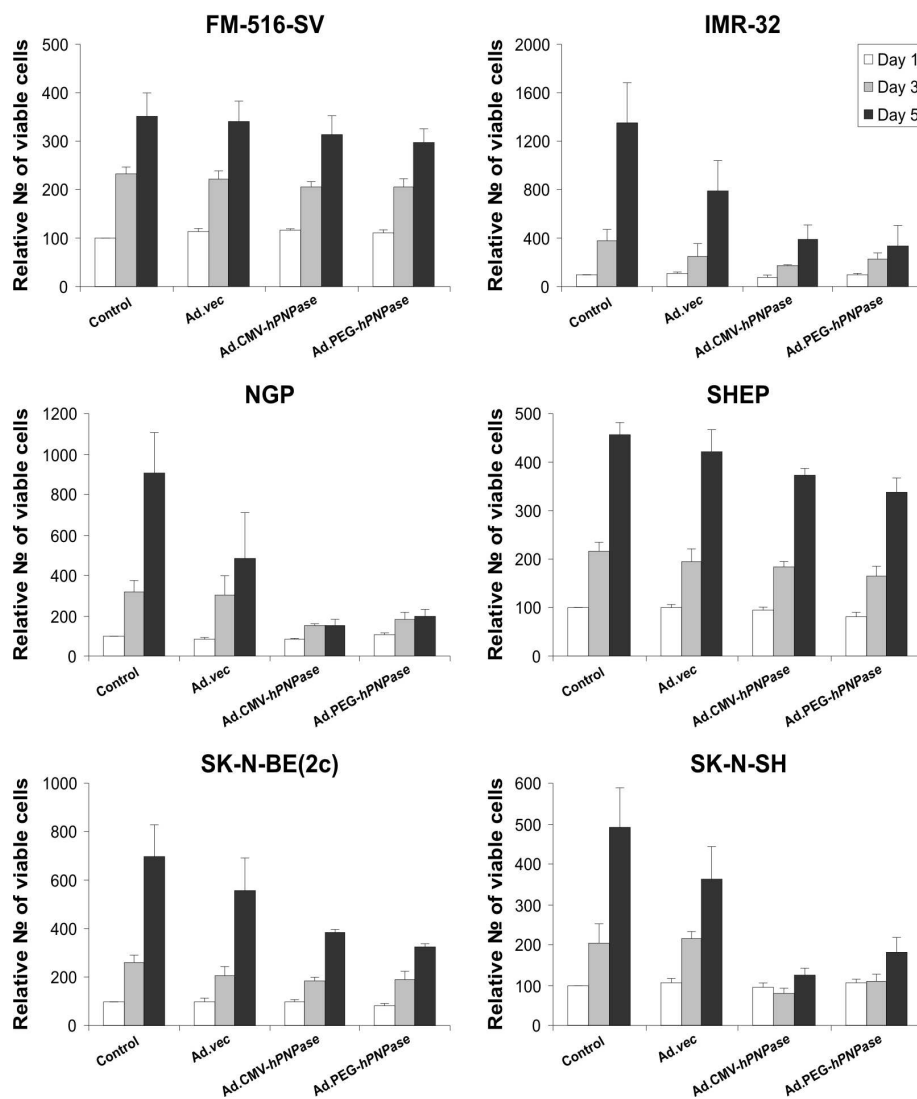
Figure 1 - Van Maerken *et al.*

128x78mm (300 x 300 DPI)

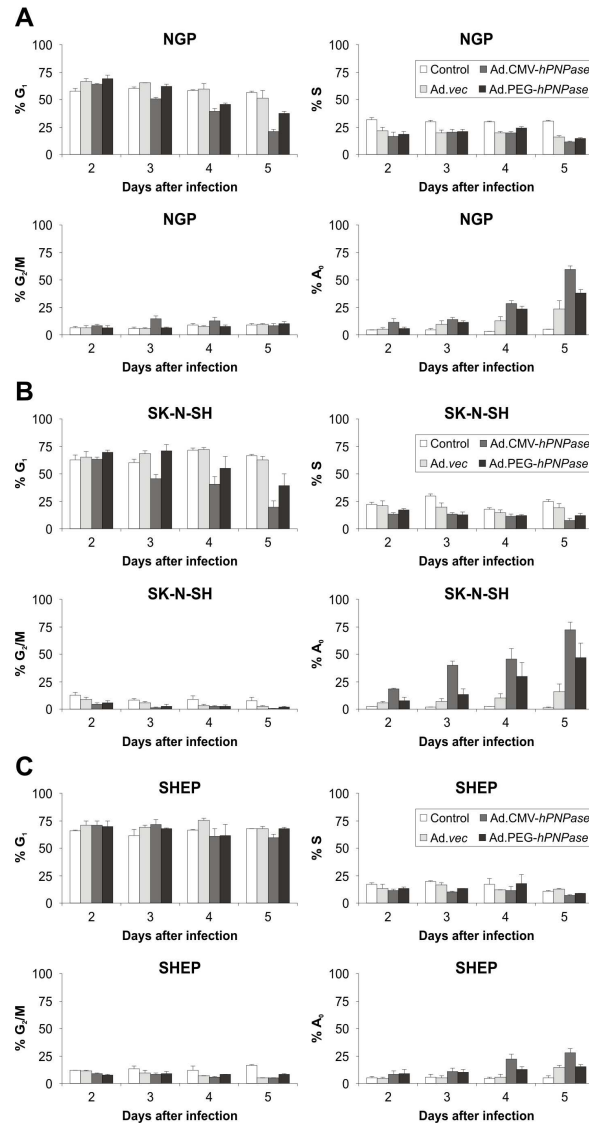
Figure 2 - Van Maerken *et al.*

111x149mm (300 x 300 DPI)

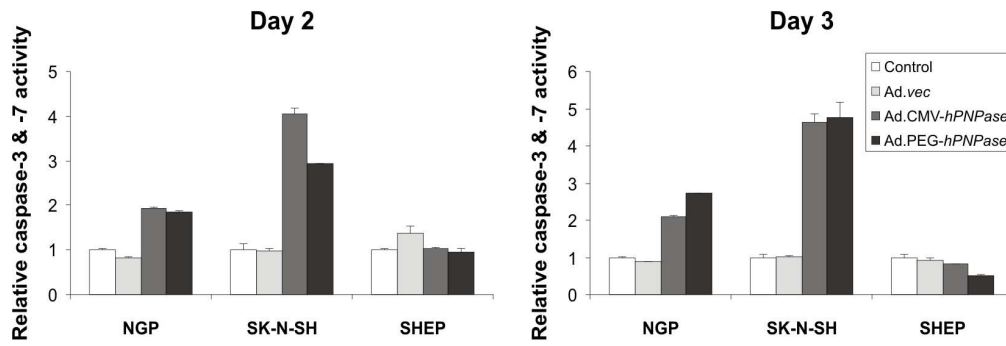
Figure 3 - Van Maerken *et al.*



135x178mm (300 x 300 DPI)

Figure 4 - Van Maerken *et al.*

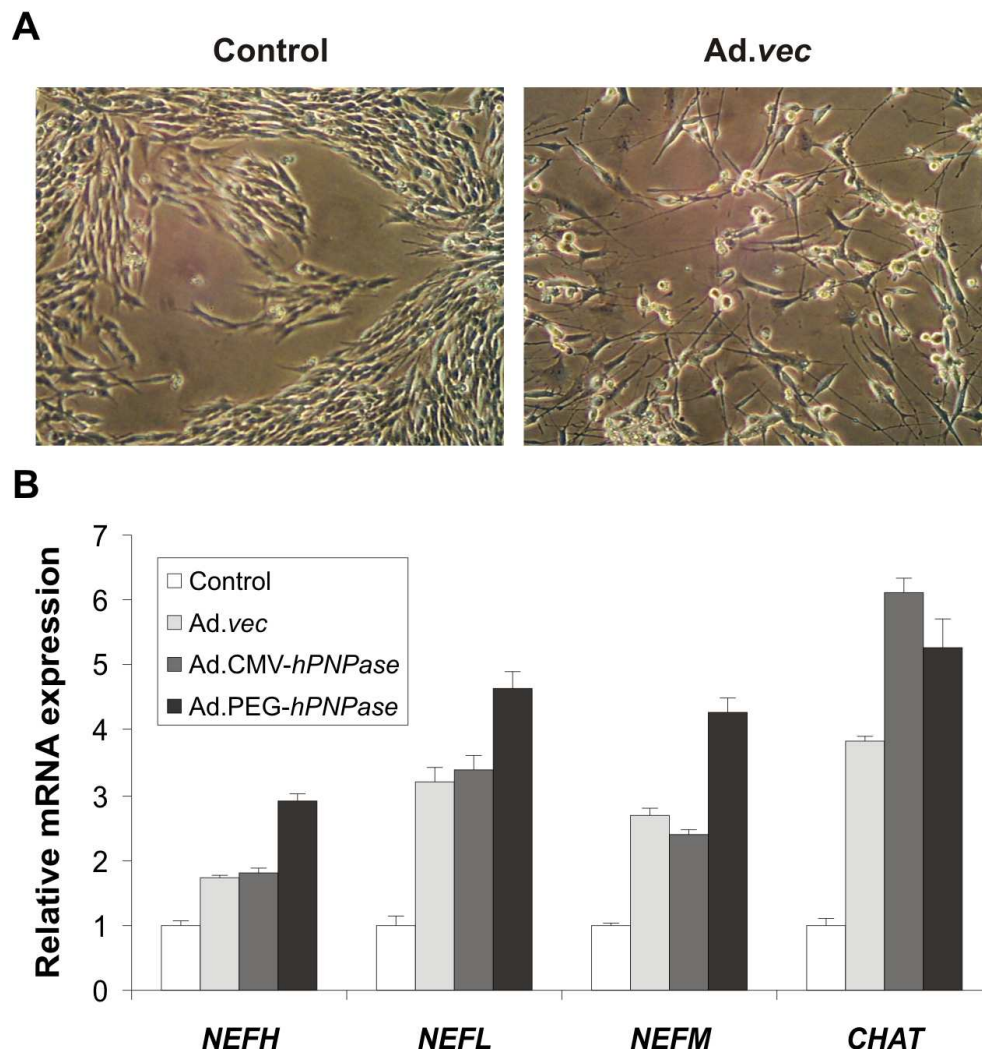
120x249mm (300 x 300 DPI)

Figure 5 - Van Maerken *et al.*

138x63mm (300 x 300 DPI)

Peer Review



Figure 6 - Van Maerken *et al.*

106x130mm (300 x 300 DPI)